CORONAL BRIGHT POINTS AT 6 cm WAVELENGTH

Q. FU*, M. R. KUNDU, and E. J. SCHMAHL

Astronomy Program, University of Mayland, College Park, MD 20742, U.S.A.

(Received 4 November, 1986)

Abstract. We report the results of the first observations of solar coronal bright points at 6 cm wavelength using the Very Large Array (VLA), with a spatial resolution of $\sim 1''.2$. The maximum brightness temperature of the sources observed is $\approx 3 \times 10^4$ K with a mean value of $\approx 1 \times 10^4$ K (above the quiet Sun value). The lifetime of most sources is between 5 and 20 min. The average diameter of the sources is about 5–15″ arc. The sources are gaussian-like near the footpoint of miniature loops and they appear in groups. The observations indicate that significant fluctuations in the brightness temperature (sometimes quasi-periodic) and in the spatial extents of these sources can occur over periods of a few minutes.

1. Introduction

Coronal bright points are the smallest scale coronal structures that have been observed on the Sun. Since their first identification in XUV and X-ray spectroheliograms (e.g., Golub *et al.*, 1974), we have learned much about their lifetime, global surface distribution, association with small bipolar magnetic regions in photospheric magnetograms, and temporal and spatial variations. Previous results relevant for this paper can be summarized as follows:

(1) The bright points are uniformly distributed on the solar surface. Typically they appear as spots of 30″–50″ in diameter.

(2) High spatial resolution studies in EUV (Sheeley and Golub, 1979; Habbal and Withbroe, 1981) show that coronal bright points appear as a collection of miniature loops or arches, a group of substructures, each typically ~ 2500 km in diameter and $\sim 12\,000$ km long.

(3) Although the mean lifetime of bright points is eight hours (Golub *et al.*, 1974), high spatial and temporal resolution studies in EUV, XUV, and X-rays show that over periods of ~ 5.5 min (the shortest time-scale available from the data of Habbal and Withbroe, 1981), there occur strong temporal and spatial variations in the emission of bright points in the chromospheric, transition region, and coronal levels, and that individual miniature loops evolve on a time-scale of ~ 6 min (Sheeley and Golub, 1979). In He 10830 Å they are observed as short lived dark features, often appearing and disappearing, and then reappearing (Harvey, 1985).

(4) The variations in the intensity of emission sometimes exhibit a quasi-oscillatory behaviour.

(5) The results of the coordinated observations by Tang *et al.* (1983) show that at any given time, there is no one-to-one correspondence between the magnetic ephemeral bipolar regions and bright points in the transition region and the corona. More

* On leave from Beijing Observatory, Beijing, Peoples Republic of China.

Solar Physics **108** (1987) 99–111.

ephemeral bipolar regions are observed than their counterparts in the upper levels of the Sun's atmosphere.

In this paper we present the results of the first observations of bright points at 6 cm wavelength using the Very Large Array (VLA). We show that at 6 cm wavelength the radio emission from bright points exhibits spatial and temporal variations similar to that observed earlier at X-ray, EUV, and optical wavelengths.

2. Observations

The observations were made on February 12, 1984 using the VLA in the *B* configuration. The array was pointed at S25E16 (heliographic coordinates at 00 UT February 12, 1984). The observations were made from $\sim 17:30$ to $19:40$ UT, interleaving solar scans (15 min) with calibration scans (4 min). The baseline coverage for the *B* array at 6 cm was $\sim 3500\,\lambda$ to $1.9 \times 10^5\,\lambda$. Therefore, the best spatial resolution for these observations was $\sim 1.2''$ arc.

There was a coronal hole near the center of the field of view (as determined from the He 10830 Å spectroheliogram of the Sun's of disk, courtesy J. Harvey), an active region (NOAA 4413) on the upper right side of the field of view and at least three other active regions on the solar disk; a few flares also occurred during and just before our observations.

Because of the lack of short baselines in the UV plane (the shortest baseline being $3500\,\lambda$), and because of the sidelobes of the sources within the field of view and some sources outside the field of view, spurious sources frequently appeared. The shortest baseline of $3500\,\lambda$ determines the spacing between the adjacent sidelobes, $\sim 50''$–$60''$ arc. Thus, the maps of many real bright points were contaminated by the effects of nearby active regions and by any flares which occurred. It is important to distinguish real sources from spurious ones.

The problem of sidelobes in this case is, fortunately, mitigated by the fact that the active regions on the Sun produced a very small response in our VLA maps. Presumably this is the result of the inability of the *B*-configuration to sample sufficiently large structures in the spot-associated sources. As a result, most of the bright point sources had brightness temperatures comparable to or exceeding the active region sources, so the maps could be CLEANed without worrying about the usual sidelobe problems associated with strong sources.

Another problem results from the use of the VLA solar calibration to determine brightness temperatures, for it has recently become well known that the standard solar calibration is unreliable. There is therefore a calibration uncertainty which we have attempted to reduce using the flux of a flare. On the day of observations, there was a small flare which we observed simultanously with Toyokawa observatory. This could, in principle, provide a good calibration for our data, were it not for the unfortunate fact that the flare occurred far outside the primary beam, where the telescope response is quite uncertain. At the present we can only suggest that our brightness temperatures are

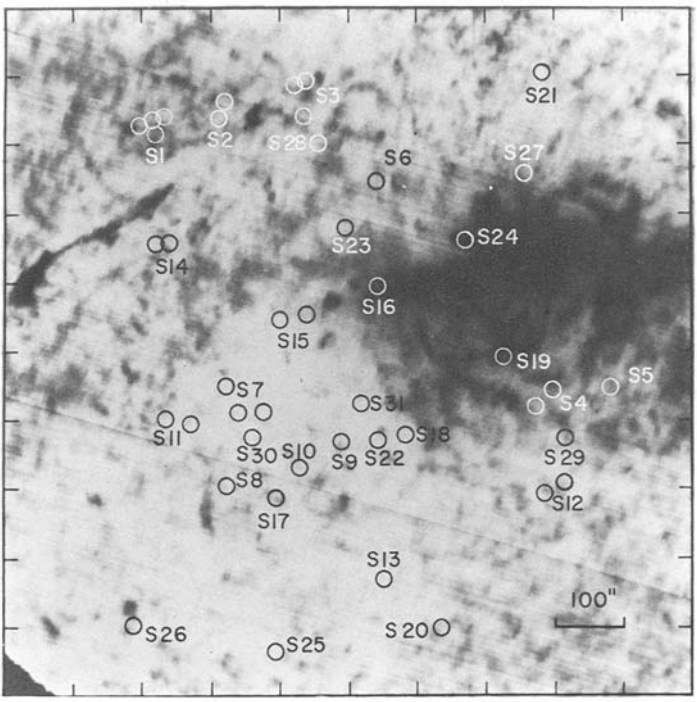

Fig. 1a. Solar coronal radio sources observed on February 12, 1984 with the VLA at $\lambda = 6$ cm, superimposed on a Kitt Peak He λ10830 spectroheliogram made at 18 : 36 UT (courtesy J. Harvey). The radio sources are shown as small circles. The sources were mapped on 31 fields, labelled S1–S31.

probably not in error by as much as a factor of two, which is smaller than the total range of observed temperatures.

The visibility data were divided into seven consecutive 15 min periods (A, B, C, D, E, F, and G). The data for period B were unavailable. Seven large maps were made using the data of the entire period of observation (2 hr) and the 15-min periods with a spatial resolution of 5″ to reduce the level of sidelobe effects. Only a few bright radio sources appeared on the 2-hr large map and the 15-min maps. Since our objective was to detect changes in emission over time-scales of minutes, we made twenty nine 3-min maps, using a 'clean' procedure with a cell size different from the larger maps. We also made nine 1-min maps for period A. Since aliasing in the maps was a serious problem, we had to test for its existence in each map. The simplest way to tell if an image is aliased is to remap the field with a different cell size; the aliased source will appear to move while a real source will stay at the same angular distance from the field center (Sramek, 1982). We accurately measured the positions of every source relative to the center of the field of view in two maps (15-min map and 3-min map), respectively, and compared their positions in the two maps. The sources were considered real if the positional shifts were less than the measurement error ($\sim 5''$); otherwise they were considered to be spurious. By following this procedure we may have missed some

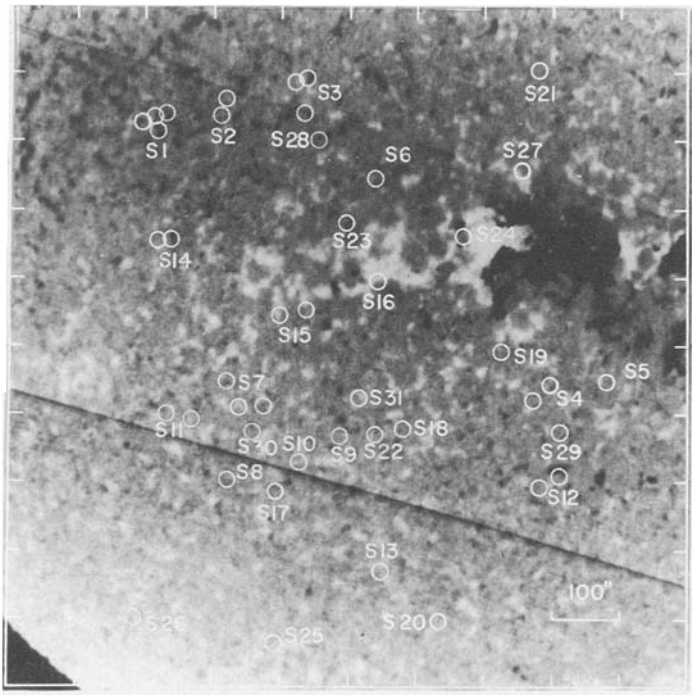

Fig. 1b. Same as Figure 1a on a magnetogram made at 16 : 47 UT (courtesy J. Harvey).

short-lived (< 3–6 min) sources; however, no other method appeared to provide enough confidence of the reality of the detected sources. Once the sources were established, their brightness temperature, diameter, position and their variation with time were determined. We made polarization (V) maps for parts of some 15-min periods, but most of the sources appeared to have no polarization.

3. Statistical Characteristics

A total of forty-four sources were detected during the two hour period of observation. The brightness temperature of the sources observed varied between 0.2×10^4 and 3×10^4 K (above the quiet Sun background). The diameters of the sources were $\sim 5''$–$16''$ arc. These temperatures and sizes are similar to those of the quiet Sun sources observed by Kundu *et al.* (1979) and Erskine and Kundu (1982). The sources were gaussian-like with no resolved fine structures. Specific features are summarized in the following.

3.1. Optical associations

We superposed the 6 cm bright points on a He 10830 Å spectroheliogram (18 : 36 UT) (courtesy of J. Harvey), as shown in Figure 1(a). The 44 radio sources are distributed

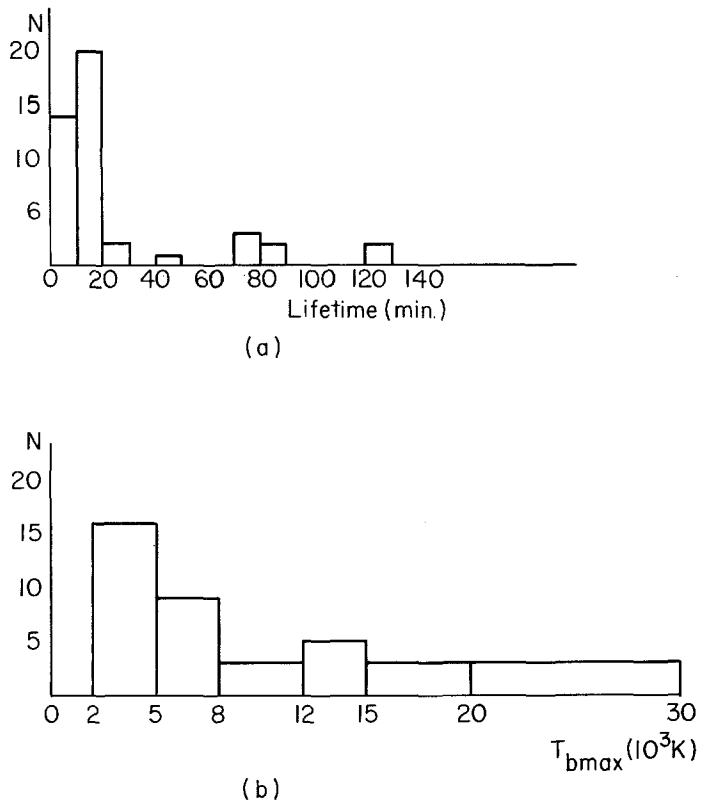

Fig. 2. Histograms of lifetime (a) and peak brightness temperature (b) for the 44 6 cm bright points.

almost uniformly on the solar disk. They were mapped in 31 groups, labelled S1–S31. Twelve out of the 44 sources in these fields coincide with, or are less than 20″ arc away from, dark He 10830 Å features. Twenty seven out of the 44 sources are associated with weak dark He 10830 Å features at distances less than 40″. However, there are many more HeI dark features without counterparts at 6 cm.

Figure 1(b) shows the same sources (17 : 30–19 : 40 UT) superposed on a KPNO magnetogram (16 : 47 UT), obtained by courtesy of J. Harvey. There do not appear to be any strong bipolar features underlying the radio bright points. This may be due to the fact the magnetogram is for an earlier time than the radio measurements. Since the lifetimes of the 6 cm bright points are less than 30 min, one might expect a poor correlation between short-lived magnetic features and 6 cm bright points, but we were unable to explore this possibility without access to other magnetograms at later times.

3.2. Distributions of Lifetime and Brightness Temperatures

Figure 2(a) shows the distribution of the lifetime of 6 cm bright points. About 86% of all bright points have lifetimes of less than 30 min. The mean lifetime is 21 min. The

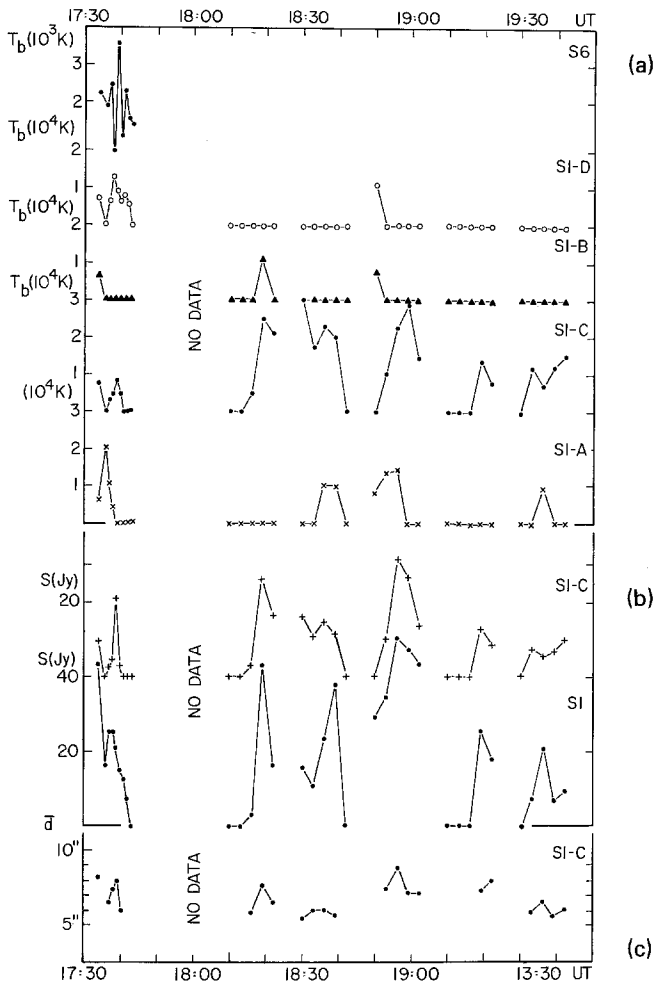

Fig. 3. Parameters for the sources of group S1 (composed of S1–A, S1–B, S1–C, and S1–D). (a) The variation of brightness temperature T_b in time for individual sources in fields S1 and S6. (b) Total flux density for source group S1 and for source S1–C. (c) The geometric average diameter $\bar{d}$ of S1–C.

number of radio bright points found in the 15-min maps were, respectively, 15, 3, 11, 9, 8, and 9. The mean number of bright points per 15-min map was about 9. From these results, we can estimate that there will be more than three hundred 6 cm bright points on the entire solar disk with two hours integrated time and ~ 70 bright points with 15 min integrated time.

Figure 2(b) shows a histogram of the peak brightness temperature of the bright points. About 65% of the bright points have peak brightness temperature of more than 8000 K (above the quiet Sun value). The mean peak brightness temperature for all bright points was 8600 K.

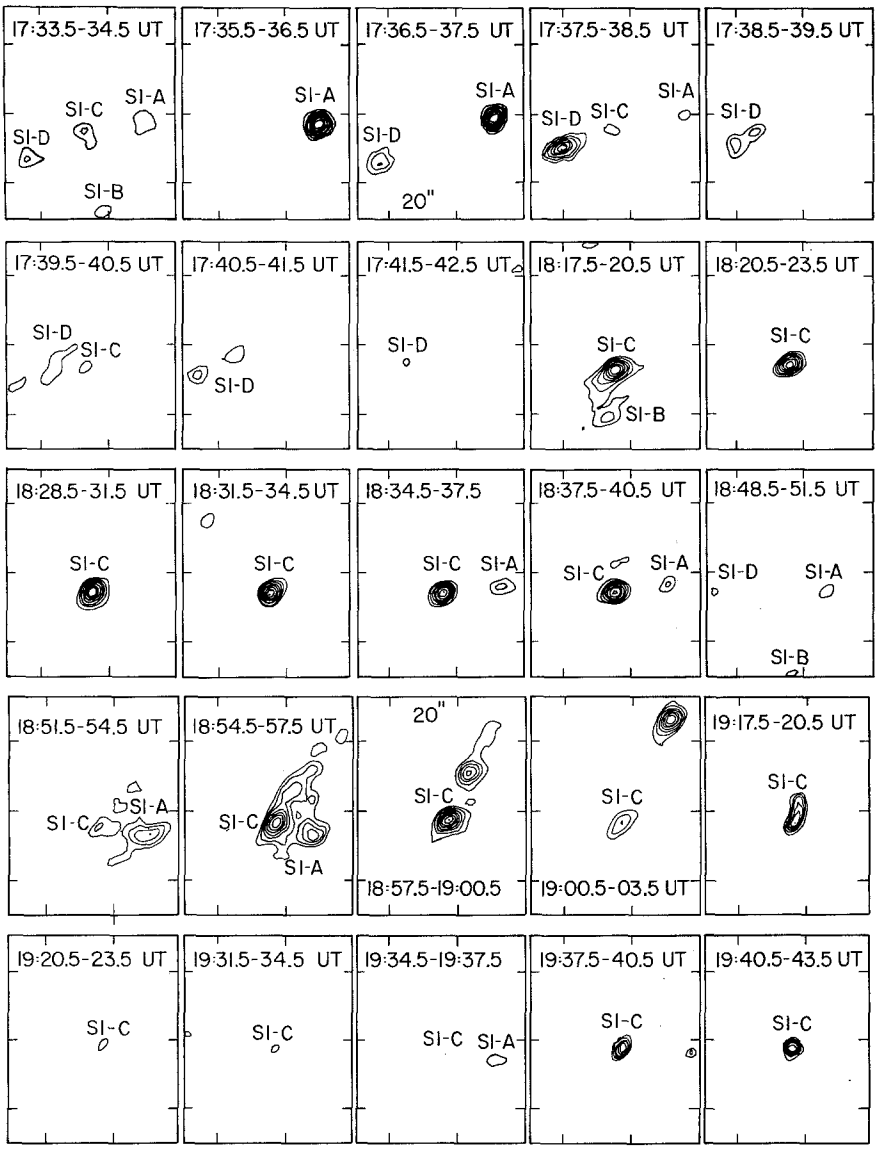

Fig. 4. Sequences of 1-min maps (17 : 33–17 : 42 UT) and 3-min maps (18 : 17–19 : 40 UT) for source S1. The tick marks around the map are spaced at 20″.

3.3. BRIGHTNESS VARIATIONS

Figure 3(a) shows plots of brightness temperature versus time for the bright points of group S1 and S6. It is clear that significant changes in the brightness temperature can occur over a few minutes. A bright point may appear for a while, disappear, and then reappear. This may repeat, as shown for the source S6 (Figure 3(a)).

Figure 3(b) shows the total flux density for the whole group S1 and for source S1–C. Figure 3(c) shows the average diameter for S1–C. From 17 : 33 to 17 : 43 UT the

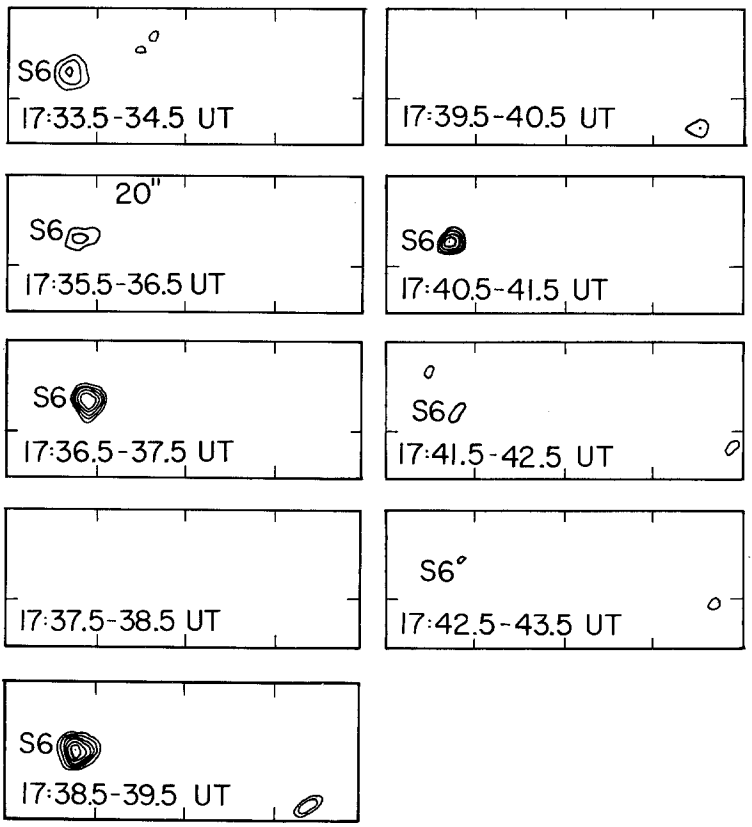

Fig. 5. The oscillation in the source S6; a sequence of 1-min maps.

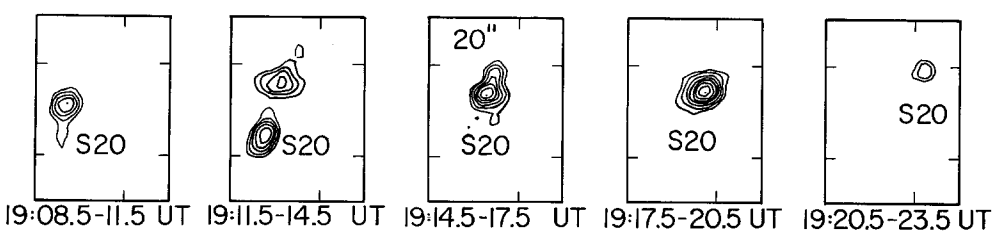

Fig. 6. Spatial variation of a 6 cm bright point: a split occurring in source S20.

parameters are from 1-min maps, and in the other time-intervals, from 3-min maps. The blank sections are data gaps. A glance at these plots shows that there are no obvious relationships between these sources. But source S1–C appears and reappears at least five times with durations of 10 to 29 nine min, during the observation time of 130 min. There are counterparts for four out of five appearances at S1–A: the peaks of S1–A appear to precede those for S1–C by 0–3 min.

Figure 4 shows sequential 1-min maps (17 : 35.5–17 : 41.5 UT) and 3-min maps of

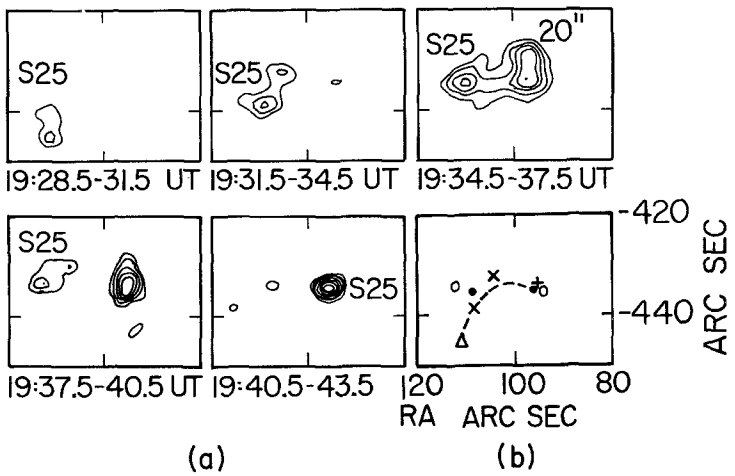

Fig. 7. Spatial variation in source S25. (a) Sequence of the 3-min maps for S25. The source moved from the lower left of the field to the right center. (b) The positions of S25 during five time intervals: 19 : 28.5–31.5 UT, △; 19 : 31.5–34.5 UT, ×; 19 : 34.5–37.5 UT, ●; 19 : 37.5–40.5 UT, ○; 19 : 40.5–43.5 UT, +.

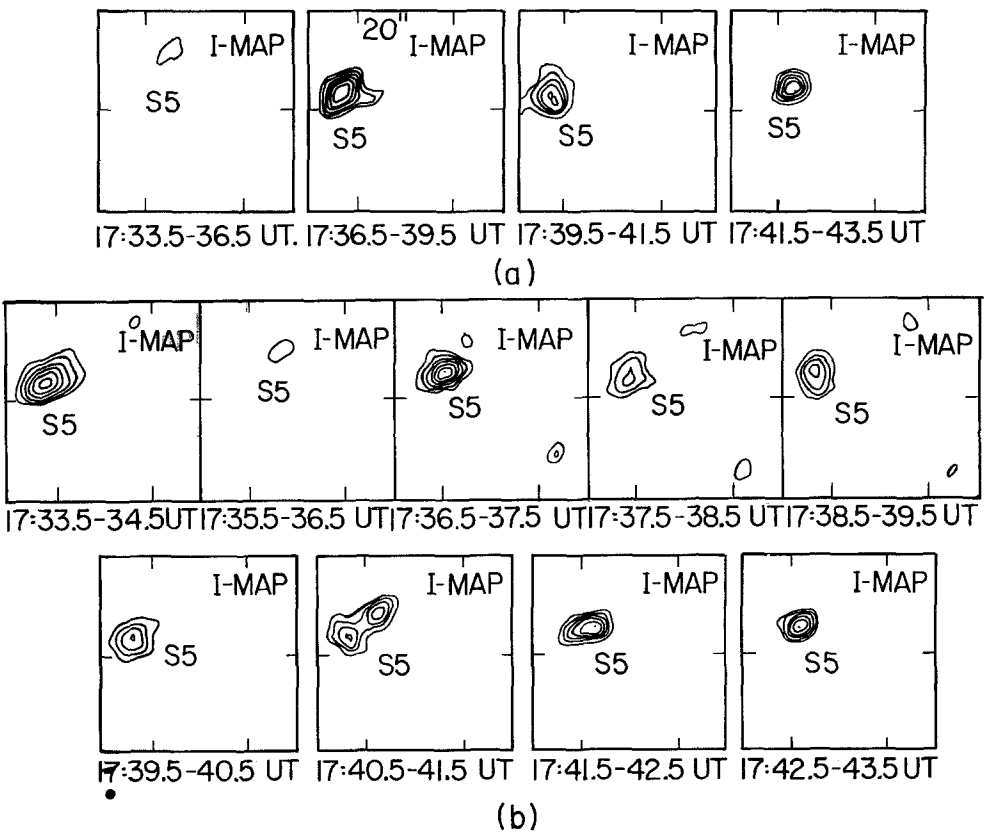

Fig. 8. (a) Sequence of 3-min of intensity maps for source S5. (b) Sequence of 1-min maps of source S5.

group S1 and Figure 5 shows sequential 1-min maps of S6. Figure 5 shows the variation of source S6, with a quasi-oscillation of about two minute period. When it was at its brightest (17 : 38.5 UT), a weak source appeared 50″ away. It is possible that this weak source lies at the footpoint of a loop connected to S6.

3.4. Spatial variations

Significant changes in the spatial extent of the sources can occur over a few minutes. Sometimes this change appears as irregular movement, and sometimes as structural change (Figure 6). For example, one part of a bright point (Figure 6) disappears while another grows and decays with time or splits into two separate parts. The size of a bright point changes with the variation in its emission. Indeed, there appears to be an inverse correlation between the brightness temperature and the diameter of a bright point. For example, see Figures 3(a) and 3(c), which show the temperature (a) and size (c) of source S–1C during intervals 18 : 30–18 : 33, 18 : 56–19 : 02, 19 : 19–19 : 22, and 19 : 33–19 : 42 UT. As previously suggested, the bright points seem to occur in groups. After disappearing for a few minutes, they reappear at the same place or near the previous positions to form a group with a size of ~30″–50″ (e.g., the sources, S–1A, S–1B, S–1C, S–1D; S–2A, S–2B; S–7A, S–7B, S–7C).

Figures 7(a) and 7(b) show an interesting phenomenon in a sequence of 3-min intensity maps for source S25. The source moved from the lower left of the field to the right center, tracing a curved arc more than 16000 km long. Figure 7(b) shows the variation of the source positions, indicating the trace by dashes. Unfortunately, no polarization map was available, but the dashed curve suggests that there was a miniature loop traced out by the 6 cm source. The inferred loop had a cross section smaller near the footpoints and larger near the top. defining the border of loops by the half power points, we find that the diameter of the cross-section was about 3500 km near the footpoint and 7500 km near the top. The 6 cm source appeared to move along the

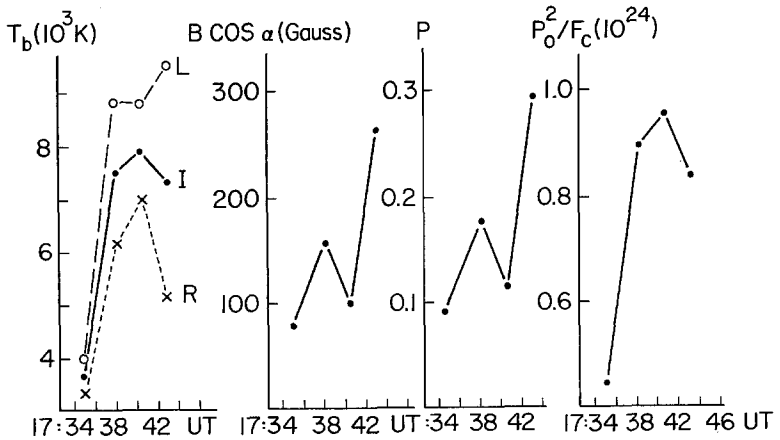

Fig. 9. The T_b, T_{bL}, T_{bR}, $B\cos\alpha$, polarization degree P and ratio P_0^2/F_c as a function of time in source S5 for a coronal temperature $T_{max} = 10^6$ K.

inferred loop with a speed of 26–48 km s^{-1}. It is also possible that there were two small loops brightening successively, the first one on the left, the second one on the right.

3.5. POLARIZATION

Most of the 24 sources for which V-maps have been made showed no significant ($\lesssim 10\%$) circular polarization. Four sources lay above unipolar regions, either negative or positive. The degree of polarization at the position of maximum brightness temperature was $\sim 30\%$ and changed significantly over a few minutes.

Habbal *et al.* (1986) defined a polarization parameter

$$a_{x,0} = \frac{7.7 \times 10^{-6}}{\omega^2 \left(1 \mp \frac{\omega_B}{\omega} |\cos \alpha|\right)^2} \frac{P_0^2}{F_c}, \tag{4}$$

where P_0 = gas pressure (K cm^{-3}), F_c = conductive flux (erg cm^{-2} s^{-1}), ω = observing frequency in Hz, ω_B = gyrofrequency, α = angle between the magnetic field and line-of-sight. Assuming T_L (the temperature at which $\omega = \omega_L$, ω_L the plasma frequency) $\ll T_{\max}$ (coronal temperature), they get the very simple and useful relations (Equation (11) in their paper):

$$a_x = \frac{T_{bx}}{T_{\max} - T_{bx}}, \tag{5a}$$

$$a_0 = \frac{T_{bo}}{T_{\max} - T_{bo}}; \tag{5b}$$

T_{bx} and T_{bo} are the brightness temperatures for the extraordinary and ordinary modes. $T_{bx} = T_{bR}$, $T_{bo} = T_{bL}$ for positive polarity. We choose $T_{\max} = 10^6$ K. Since most of the sources had no significant polarization, $T_{bx} = T_{bo}$. Using the observed mean brightness temperature of 8600 K, P_0^2/F_c is $\sim 1.1 \times 10^{24}$ K^2 erg^{-1} cm^{-4} s.

For four bright points which have measurable polarization, we find that the minimum field strength varied between 40 and 400 G, with an average field of ~ 130 G. We also find that the average value of $P_0^2/F_c \sim 0.52 \times 10^{24}$ K^2 erg^{-1} cm^{-4} s.

Figure 8(a)–(b) shows the sequence of 3-min and 1-min intensity maps of S5. The shift of the intensity maximum (17 : 39.5–17 : 42.5) suggests that the radio bright points at 6 cm were located above the footpoints of a magnetic loop. Sometimes, a weak source appears above one or the other pole of the loop on the 1-min maps (Figure 8(b), 17 : 36.5, 17 : 37.5) (The shifts are smeared out on maps with longer integration time.) The small magnetic field configuration changed from 1 min to the next and the source split happened within one minute (Figure 8(b), 17 : 40.5). Figure 9 illustrates the variation of the parameters T_{bI}, T_{bR}, T_{bL}, $B \cos \alpha$, P, and P_0^2/F_c as a function of time for S5, using Equations (4) and (5).

4. Discussion and Conclusions

We have presented the results of observations and analysis of coronal bright points at 6 cm wavelength. Many of the properties of bright points at 6 cm wavelength appear to be similar to those observed at 20 cm, EUV and X-ray (Habbal *et al.*, 1986; Golub *et al.*, 1974; Sheeley and Golub, 1979; Habbal and Withbroe, 1981). There are, however, differences in characteristics, particularly in size and polarization.

Sheeley and Golub (1979) and Habbal and Withbroe (1981) observed that coronal bright points are groups of substructures like miniature loops; the individual substructures brighten in a more or less random fashion, with each substructure brightening up for a few minutes at a time; the life history of a bright point is a continuous sequence of rapidly evolving and independently evolving miniature loops.

The compact sources found at 6 cm wavelength with a diameter of 5″–15″ arc and a lifetime of 5–20 min may be the miniature loops, i.e., members of the substructures of bright points. From Figures 1 and 4 we can see that the source group S1 is composed of 4 members; some sources are composed of at least 2 members, such as S2, S3, S4, S7, S11, S14, ..., and so on. The size of a group is about 50″ arc, the typical size of an X-ray bright point. For a few radio sources with some possible polarization, the intensity maximum was separated from the centroid of the polarization map by ~2.″5–10″ arc. Thus it is possible that the 6 cm counterpart of a bright point is near the footpoint of a miniature loop. Possibly some of the short-duration sources are flaring bright points (Golub *et al.*, 1974).

Using the differences between the distances from the center of the solar disk to the radio sources and to the associated dark points at He λ10830 Å, we have found that the height of the 6 cm bright points is $1.5–2.0 \times 10^4$ km above the layer where He λ10830 Å is formed.

The observations that the spatial extent of a 6 cm bright point decreased while its intensity increased (and vice versa) is interesting and should be further investigated.

One remarkable feature of the 6 cm bright points is their rapid fluctuation in intensity. This may have significance for one of the fundamental and unsolved problems in solar physics, namely, coronal heating. Observations in spectral lines formed near the temperature minimum layer suggest that there is a large mechanical energy flux carried by waves having periods between 10 and 300 s. The variation in intensity of an observed radio bright point at 6 cm has a quasiperiod of about 120 s. We should note that higher temporal resolution and longer observation intervals are necessary to establish the oscillatory nature of bright point intensity variation. Also, it is important to compare such variations with high resolution video magnetograms and filtergrams, to identify the cause of the fluctuations.

The observations by Tang *et al.* (1983) indicate that at any one time there is no one-to-one correspondence between the ephemeral regions and bright points in the transition region and the corona. Our observations suggest a similar pattern. We note that there is an important difference between much larger active regions and these very small active region (ephemeral region) bright points where the photospheric magnetic

flux is distributed in relatively few elements (Sheeley and Golub, 1979), and there is a lack of a strong enough magnetic field to link up the whole layer of solar atmosphere. More ephemeral regions at the photospheric level are observed than their counterparts in the upper atmosphere, in particular at radio wavelengths. It will be interesting to find the difference between the ephemeral bipolar regions (or the dark points at He 10830 Å spectroheliograms) associated with radio bright points and those not associated. The radio observations permit the investigation of bright points at different levels of the Sun's atmosphere with a temporal resolution (of ~ 1 min), and a spatial resolution of a few arc sec. They show many aspects of the small scale structures of the corona that require further study for an understanding of the physical processes involved.

Acknowledgements

This research was supported by NSF grant ATM 84–15388 and NASA grant NGR 21–002–199 and NASA contract NAG–5511. We thank Dr Jack Harvey for providing us with the magnetogram and He 10830 Å spectroheliogram, and indicating to us the location of bright points and coronal holes on a He 10830 Å spectroheliogram of the Sun taken on February 12, 1984. The National Radio Astronomy Observatory is operated by Associated Universities Inc., under contract with the National Science Foundation.

References

Erskine, F. and Kundu, M. R.: 1982, *Solar Phys.* **76**, 321.
Golub, L., Krieger, A. S., Vaiana, G. S., Silk, J. K., and Timothy, A. F.: 1974, *Astrophys. J.* **189**, L93.
Habbal, S. and Withbroe, G.: 1981, *Solar Phys.* **69**, 77.
Habbal, S., Ronan, R., Withbroe, G., Shevgaonkar, R. K., and Kundu, M. R.: 1986, *Astrophys. J.* **306**, 740.
Harvey, K.: 1985, *Australian J. Phys.* **38**, 875.
Kundu, M. R., Rao, A., Erskine, F., and Bregman, J.: 1979, *Astrophys. J.* **234**, 1122.
Sheeley, N. and Golub, L.: 1979, *Solar Phys.* **63**, 119.
Sramek, R.: 1982, in A. R. Thompson and L. R.D'Addario (eds.), *Synthesis Mapping, Proceedings of the NRAO-VLA Workshop*, held at Socorro, New Mexico, June 21–25, 1982, pp. 2–4.
Tang, F., Harvey, K., Bruner, M., Kent, B., and Antonucci, E.: 1983, *Adv. Space Res.* **2**, 65.
Withbroe, G. and Noyes, R.: 1977, *Ann. Rev. Astron. Astrophys.* **15**, 363.